

# Metal Adsorption Property of Succinamic Acid Functionalized MCM-41

Aneesh Mathew

Reaction & Separation Nanomaterials Laboratory, Graduate School of Energy Science and Technology,  
Chungnam National University Yuseong-gu, Daejeon 34134, Republic of Korea

Surendran Parambadath\*

Department of Chemistry,  
T M Jacob Memorial Govt. College, Manimalakunnu, Ernakulam, India

## Abstract

The adsorption properties of succinamic acid functionalized MCM-41 (SA-MCM-41) towards transition metals was investigated. The material was synthesized initially by anchoring (3-aminopropyl)triethoxysilane (APTES) over MCM-41 (A-MCM-41), and the proceeding immobilization of succinic anhydride in hot methanol (SA-MCM-41). X-ray diffraction and transmission electron microscopy showed that the MCM-41, A-MCM-41 and SA-MCM-41 materials had mesoscopically ordered, hexagonal symmetry and well-defined morphologies. The  $N_2$  sorption experiments showed that the material has a large surface area ( $1008 \text{ m}^2 \text{ g}^{-1}$ ), acceptable pore diameter (2.8 nm) and reasonable pore volume ( $0.54 \text{ cm}^3 \text{ g}^{-1}$ ) which is suitable for maximum functionalization.  $^{29}\text{Si}$  magic angle spinning nuclear magnetic resonance (MAS NMR) spectroscopy revealed a change in the silicon environment by each step of modification. Organic functionalization was determined successfully by Fourier transform infrared and  $^{13}\text{C}$  cross-polarisation magic angle spinning (CP-MAS) nuclear magnetic resonance (NMR) spectroscopy. The optimal condition for the removal of  $\text{Cr}^{3+}$ ,  $\text{Co}^{2+}$ ,  $\text{Ni}^{2+}$ ,  $\text{Cu}^{2+}$  and  $\text{Cd}^{2+}$  from water was explored by varying the parameters, such as solution concentration, initial pH, stirring time, and amount of adsorbent. The adsorbent exhibited low adsorption ability towards the individual metal ion solutions under our experimental condition. SA-MCM-41 was shown exceptional amount of adsorption for  $\text{Cr}^{3+}$  and  $\text{Cu}^{2+}$  ions from the five metal mixture at pH 6.5. The effect of the metal ion concentration over mole adsorption selectivity in the ternary mixture was examined by doubling the concentration of at least one metal ion in the mixture. The result was compared with the ternary mixture containing equal concentrations of metal ions.

## Keywords

Mesoporous, MCM-41, Succinamic acid, Adsorption, Metal ions.

## I. INTRODUCTION

The discovery of mesoporous silica, M41S family in 1990 by the mobile researchers has stimulated a renewed interest in adsorbents and catalysts design to modify the material for environment cleaning [1-4]. MCM-41 as one of the members in this family possesses high surface area, crystallinity, thermal stability, tunable morphology, and uniform pore size ranging from 2 to 10 nm and the availability of Si-OH group on the material surface provides the possibility to tailor different variety of silane functionality [4-6]. For environmental remediation, adsorption of metal ions is getting much attention with the techniques like, ion exchange, reverse osmosis, nanofiltration, precipitation, electrolysis, chemical oxidation, disinfection, foam flotation, membrane process, coagulation and co-precipitation [7-9]. The adsorption process offers flexibility in design and operation in many cases will produce high-quality treated effluent. Various adsorptive compounds, such as activated charcoal, activated alumina, silica gel, molecular sieve carbon, metal oxides, molecular sieve zeolites, clays and polymeric adsorbents are capable of capturing metal ions from aqueous solutions. MCM-41 functionalized with various chelating agents is increasingly utilized as an adsorbent because of its high selectivity or amount of adsorption [10]. The removal of highly toxic heavy metal pollutants, from water sources is an important task to clean up our environment. Rapid industrialization has seriously contributed to the release of toxic heavy metals to water streams. Mining, electroplating, metal processing, textile, and battery manufacturing industries are the major sources of heavy metal ions contamination. The removal of metal ions from the contaminated water is required, before discharging to the environment. The addition of organic groups by grafting of organosiloxane precursors onto the surface of the silica pore results in functional mesoporous hybrid materials. The usage of such hybrid materials in this revolutionary endeavor is more attractive due to the

chance of tuning the support as well as ligand for some confined aims. Moreover, this modification of adsorbents with organic functional groups has been shown to improve the selectivity of the adsorbents for binding desired metal ions and has recently drawn much attention. The high removal efficiency of such adsorbents is the main advantage over traditional adsorbents. These organic-inorganic hybrid materials have been reported to exhibit improved sorption properties towards heavy metal ions, superior to those achieved with silica gel functionalized with the same ligand [11].

The organic functionalization of these mesoporous inorganic materials has generated considerable attention because of the attractiveness of combining a wide range of organic compound properties with the robust thermal and mechanical stabilities of inorganic solids. So far, two main pathways are available for functionalization of mesoporous silica materials with organic groups. The co-condensation of tetraalkoxysilanes with terminal trialkoxy organosilanes in the presence of structure-directing agents is an effective method for getting surface functionalized mesoporous materials [12, 13]. Another approach for the surface functionalization is the grafting method based on direct reaction between organosilane and surface silanols [14, 15]. We adopted the grafting method for the effective surface functionalization of MCM-41 in this study.

The objectives of the present study is to evaluate the metal adsorption capacity of the succinamic acid modified MCM-41 in the adsorption of  $\text{Cd}^{2+}$ ,  $\text{Co}^{2+}$ ,  $\text{Ni}^{2+}$ ,  $\text{Cu}^{2+}$ , and  $\text{Cr}^{3+}$  as model metal ions, as well as investigate the factors affecting the amount of adsorption of metals. The detailed synthesis and characterization of succinamic acid functionalized MCM-41 has been discussed in our previous report [16].

## II. EXPERIMENTAL

### A. Chemicals

Cetyltrimethylammoniumbromide (CTAB), tetraethyl orthosilicate (TEOS), (3-aminopropyl)triethoxysilane (APTES), succinic anhydride (SA), cadmium nitrate tetrahydrate  $\text{Cd}(\text{NO}_3)_2 \cdot 4\text{H}_2\text{O}$ , cobalt nitrate hexahydrate  $\text{Co}(\text{NO}_3)_2 \cdot 6\text{H}_2\text{O}$ , nickel nitrate hexahydrate  $\text{Ni}(\text{NO}_3)_2 \cdot 6\text{H}_2\text{O}$ , copper nitrate hexahydrate  $\text{Cu}(\text{NO}_3)_2 \cdot 6\text{H}_2\text{O}$ , chromium nitrate nonahydrate  $\text{Cr}(\text{NO}_3)_3 \cdot 9\text{H}_2\text{O}$ , and dry toluene were used as received from Aldrich.

### B. Synthesis of MCM-41

MCM-41 was synthesized using CTAB as the structure directing agent and TEOS as the silica source. The reaction procedure was as follows: CTAB (0.5 g, 1.4 mmol) and an ammonia solution (26.7 g, 27 %) were placed in distilled water (105 g). The mixture was stirred for 30 min at 50 °C in an oil bath. TEOS (2.35 g, 11 mmol) was then added

drop wise to the clear solution. The mixture was allowed to stir for a further 3 h at 75 °C, the white precipitate was separated by filtration and washed well with deionized water and ethanol. The obtained material was dried at 50 °C under vacuum overnight. Surfactant removal was carried out by calcination at 550 °C for 6 h at a heating rate of 1 °C  $\text{min}^{-1}$  [17, 18].

### C. Preparation of amino-functionalized MCM-41 (A-MCM-41)

The silanization of MCM-41 by APTES was carried out using the grafting method reported elsewhere [16, 19]. Briefly, MCM-41 (1 g) was heated with APTES (1 g, 4.51 mmol) in dry toluene (100 ml) for 24 h under reflux. The solid product was filtered off and washed with toluene, ethanol and dried in an oven at 50 °C for overnight. The material obtained was labelled A-MCM-41 [16].

### D. Preparation of succinamic acid tailored MCM-41 (SA-MCM-41)

Carboxyl groups were introduced quantitatively onto A-MCM-41 via a ring-opening reaction of succinic anhydride (SA) with A-MCM-41 [16, 20]. Briefly, A-MCM-41 (1 g) was heated to 60 °C with SA (1.32 g, 13.2 mmol) in dry toluene under a nitrogen atmosphere in the presence of TEA (2 mmol). 1:2 ratios for amino functionality in MCM-41 and SA were used to replace the hydrogen atoms in the amino group. After 24 h, the solid product was separated by filtration and washed several times with toluene and dichloromethane, dried under vacuum for overnight at 50 °C and labelled as SA-MCM-41 [16].

### E. Adsorption from individual metal solution

A solution of  $\text{Cr}^{3+}/\text{Cu}^{2+}/\text{Ni}^{2+}/\text{Co}^{2+}/\text{Cd}^{2+}$  ions was prepared by dissolving a known amount of the corresponding nitrate salt in distilled water. The concentration of metal ions ranged from 0.5 to 5 mM, and the adsorption experiments were conducted by suspending 0.01 g of SA-MCM-41 in 10.0 ml of metal ion of aqueous solution at pH 6.5. The effect of pH on the metal ion uptake was examined by performing equilibrium sorption experiments by varying the solution pH from 3.0 to 6.5. The solution pH was adjusted by adding either 0.1 M  $\text{HNO}_3$  or  $\text{NaOH}$ . SA-MCM-41 (0.01 g) was added to the aqueous metal solution (10.0 ml, 0.5–5.0 mM) and shaken for the desired time at 25 °C. The adsorbent was filtered out through a polypropylene microfilter, and the amount of  $\text{Cr}^{3+}/\text{Cu}^{2+}/\text{Ni}^{2+}/\text{Co}^{2+}/\text{Cd}^{2+}$  adsorbed by SA-MCM-41 was measured by ICP-AES. The amounts of metal ions adsorbed were calculated from the difference between the initial (Co) and

equilibrium (Ce) concentrations in the supernatant after centrifugation. The adsorption percentage [adsorption (%) =  $\text{Co}/(\text{Co}-\text{Ce}) \times 100$ ] was derived from the difference between Co and Ce [21-23].

#### F. Competitive adsorption from a mixture of metal ion solution

Competitive adsorption by SA-MCM-41 from 0.5 mM metal mixture of  $\text{Cr}^{3+}$ ,  $\text{Cu}^{2+}$ ,  $\text{Ni}^{2+}$ ,  $\text{Co}^{2+}$ , and  $\text{Cd}^{2+}$  ions at pH 6.5 was exposed for analyzing the metal adsorption selectivity. The solution pH was adjusted by adding a 0.1 M  $\text{HNO}_3$  or  $\text{NaOH}$  solution. 0.01 g of SA-MCM-41 was added to 10 ml of the above solution and shaken for 24 h to establish the adsorption equilibrium [10, 24]. The mixture was filtered, and the amount of metal adsorption was measured by ICP-AES analyzer.

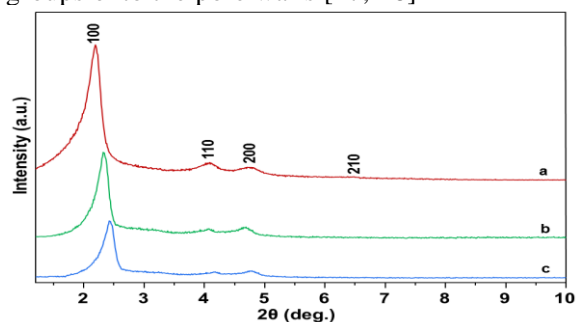
#### G. Characterization techniques

XRD (Bruker AXN) was performed using  $\text{Cu-K}\alpha$  radiation. The XRD patterns were collected over the low-angle range from  $1.2^\circ$  to  $10^\circ$   $2\theta$ . TEM (JEOL 2010) was performed at an accelerating voltage of 200 kV. The SEM (JEOL 6400) images were collected at an operating voltage of 20 kV. The  $\text{N}_2$  adsorption-desorption isotherms were measured using a Nova 4000e surface area and pore size analyser. The samples were degassed at  $120^\circ\text{C}$  for 12 h prior to the measurements. The Brunauer-Emmet-Teller (BET) method was used to calculate the specific surface area. The pore size distribution was obtained from an analysis of the adsorption branch using the Barrett-Joyner-Halenda (BJH) method. The Fourier transform infrared (FT-IR, JASCO FTIR 4100) spectra were measured from KBr pellets over the frequency range,  $4000\text{--}400\text{ cm}^{-1}$ . The  $^{13}\text{C}$  CP and  $^{29}\text{Si}$  MAS NMR (Bruker DSX 400) spectra were obtained using a 4 mm zirconia rotor spinning at 6 kHz (resonance frequencies of 79.5 and 100.6 MHz for  $^{29}\text{Si}$  and  $^{13}\text{C}$  CP MAS NMR, respectively;  $90^\circ$  pulse width of 5 ms, contact time of 2 ms, recycle delay of 3 s for both  $^{29}\text{Si}$  MAS and  $^{13}\text{C}$  CP MAS NMR, Korea Basic Science Institute, Daejeon Center). Elemental analysis for C, H and N was performed by combustion analysis on a Perkin Elmer CHN Analyser (Model 2400). The zeta potential measurements were carried out using Zetasizer Nano ZS (Malvern Instruments Ltd, Malvern, UK) fitted with a high-concentration zeta potential cell (ZEN1010). Quantitative determination of the metal ion content was performed by ICP-AES (ACTIVA, JYHORIVA, Japan).

### III. RESULTS AND DISCUSSION

#### A. Characterization of the functionalized mesoporous MCM-41

We have already reported the synthesis and characterization of succinamic acid functionalized MCM-41 and its exceptional dye adsorption property [16]. Even though, here we are discussing some of the main characterization results. The powder XRD patterns of (a) MCM-41, (b) A-MCM-41 and (c) SA-MCM-41 (Fig.1). The pattern (1a) exhibited a very sharp  $d_{100}$  diffraction peak at  $2.19^\circ$ . The indication of a well-ordered material can be observed from three additional peak of  $d_{110}$ ,  $d_{200}$  and  $d_{210}$  at lower intensities at  $4.07^\circ$ ,  $4.78^\circ$  and  $6.48^\circ$ , respectively [25]. The A-MCM-41 and SA-MCM-41 materials also exhibited the above reflections except for the  $d_{210}$  peak, indicating the maintained integrity of the mesoporous structure. Furthermore, existence of  $d_{110}$ ,  $d_{200}$  reflections indicates long range order was retained even after modification with propyl amine (Fig. 1b) and succinamic acid (Fig. 1c) [26]. A decrease in the  $d_{100}$  peak intensity and a shift to higher  $2\theta$  values after functionalization with APTES and SA indicated the expected decrease in pore diameter due to the successful loading of functional molecules in a step wise manner inside the pore channels [20]. It was reported that a slight decrease in the  $d_{100}$  values as well as a lower contrast of XRD pattern could be attributed to the covalent linkage of organic groups onto the pore walls [27, 28]



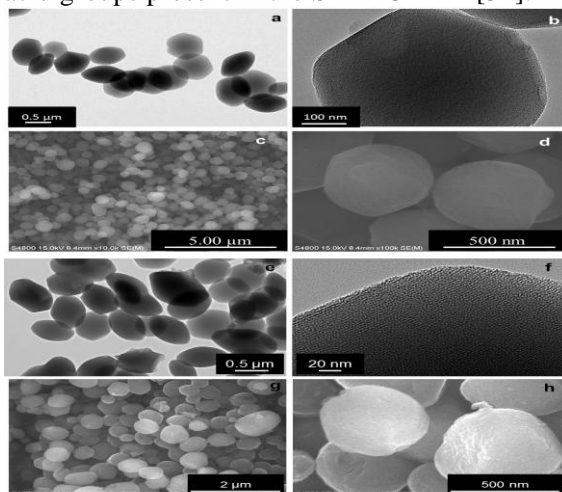
**Fig. 1. XRD patterns of (a) calcined MCM-41, (b) A-MCM-41 and (c) SA-MCM-41.**

Fig. 2 presents the representative TEM and SEM images of MCM-41 and SA-MCM-41. TEM images of MCM-41 (a, b) and SA-MCM-41 (e, f) revealed hexagonal crystalline growth and well defined pore channels with long range order to the cylindrical pores. The scanning electron microscopy (SEM) images of the MCM-41 (c, d) and SA-MCM-41 (g, h) materials resemble the formation of well-defined polyhedral particles without intergrowth aggregation. The particle size of the synthesized material varies from 600 to 1000 nm and the mean particle size was about 700 nm. TEM and SEM analysis revealed the hexagonal crystalline growth and well defined

pore channels with long range order to the cylindrical pores [3].

The FTIR spectra of MCM-41 before and after modifications are giving the functional information (Fig. 3). In all samples, a broad and strong band between 3700 and 3200  $\text{cm}^{-1}$  was observed, corresponding to the O-H stretching vibration of adsorbed water molecules and hydrogen bonded surface silanol groups in the MCM-41 matrix. The major peaks of MCM-41 (Fig. 3a) were 1085 (asymmetric Si-O-Si stretching), 959 (Si-OH stretching), 799 (symmetric Si-O-Si stretching), and 458  $\text{cm}^{-1}$  (Si-O-Si bending) [29]. The broad peak was positioned at 1636  $\text{cm}^{-1}$  in MCM-41 is the bending vibration of adsorbed water molecule. After APTES functionalization (Fig. 3b), the stretching and bending vibrations of aliphatic C-H groups at 2934 and 2857  $\text{cm}^{-1}$ , respectively, were appeared [30]. A weak band at 692  $\text{cm}^{-1}$ , corresponds to the out of plane bending vibration of a C-H group, highlights the existence of propyl amine [31]. The small and strong band observed at 1559  $\text{cm}^{-1}$  is assigned to the -NH scissoring vibration, which indicates the existence of the primary amine in the material [32]. The presence N-H group was evidenced from the absorption bands at 1635 and 3400  $\text{cm}^{-1}$ , whereas the relatively broad peaks at 780 and 1160  $\text{cm}^{-1}$  indicate the presence of an N-H wagging vibration and the anti-symmetrical stretching vibration of the C-N-C moiety, respectively [33].

The formation of succinamic acid is evidenced from the representing vibrations in the spectra of SA-MCM-41 (Fig. 3c). Similarly, in the previous spectra, the vibrations for silica material were observed at 458, 801, 960, and 1085  $\text{cm}^{-1}$ . The band at 1716  $\text{cm}^{-1}$  was assigned to the C=O stretching mode of the carboxylic acid groups present in the SA-MCM-41 [34].



**Fig. 2.** TEM images of MCM-41 (a and b) and SA-MCM-41 (e and f) and SEM images of MCM-41 (c and d) and SA-MCM-41 (g and h).

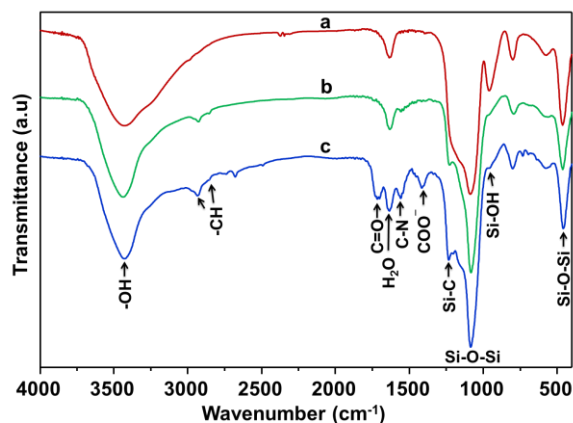


**Fig. 3.** FT-IR spectra of (a) MCM-41, (b) A-MCM-41 and (c) SA-MCM-41.

The adsorption peaks centered at 1635, 1563 and 1416  $\text{cm}^{-1}$  were attributed to C=O, NH and C-N bands, respectively, of amide vibrations of the carboxylate group and the methylene bending vibration of the  $\alpha$ -CH<sub>2</sub> group [35]. These observations from the three spectral lines were attributed to the successful formation of succinamic acid over MCM-41. The band near 1416  $\text{cm}^{-1}$  was assigned to a strong coupling between the symmetric stretching vibrations of the carboxylate group and the methylene bending vibration of the  $\alpha$ -CH<sub>2</sub> group [36, 37]. These observations from the three spectral lines were attributed to the successful formation of succinamic acid over MCM-41.

Fig. 4 represents the <sup>29</sup>Si MAS NMR spectra of (a) calcined MCM-41 and (b) A-MCM-41 materials. Two groups of signals could be distinguished in the spectra, (a) Q signals from silicon atoms without organic substitution and (b) T signals related to organo-substituted silicon. MCM-41 (Fig. 4a) showed three 'Q' signals due to SiO<sub>2</sub>(OH)<sub>2</sub> (Q<sup>2</sup> sites) at -90 ppm, SiO<sub>3</sub>-OH (Q<sup>3</sup> sites) at -100 ppm and SiO<sub>4</sub> (Q<sup>4</sup> sites) at -110 ppm were observed. The most intense peak in the spectra was Q<sup>3</sup>, which suggests the presence of enough surface silanol groups for functionalization, as expected from the MCM-41 type material. The intensity of the Q<sup>4</sup> peak was also considerable compared to the intensity of Q<sup>3</sup> and Q<sup>2</sup>, which deliver the idea about the formation of porous material with a highly cross linked silica framework. After functionalization with the propyl amine group, additional broad and overlapping signals appeared in the spectrum (Fig. 4b) at  $\delta \approx -51$  and  $-56$  ppm, which were assigned to T<sup>2</sup>[(SiO)<sub>2</sub>(OH)SiC] and T<sup>3</sup>[(SiO)<sub>3</sub>SiC] organosilica environment, respectively, with T<sup>3</sup> as the major peak [38]. The intensity of the signal corresponding to T<sup>3</sup> species was approximately double that of the T<sup>2</sup> species. This suggests that in the

functionalisation process, the APTES group was bound more tightly in the bulk and over the outer surfaces of MCM-41.

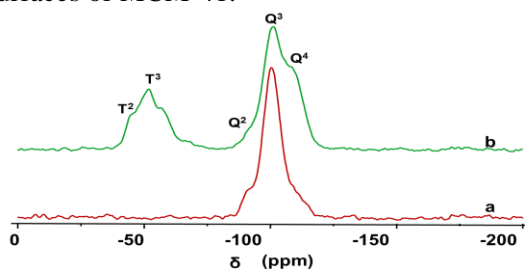


Fig. 4.  $^{29}\text{Si}$  MAS NMR spectra of (a) MCM-41 and (b) A-MCM-41.

The  $^{13}\text{C}$  CP MAS NMR spectra of (a) A-MCM-41 and (b) SA-MCM-41 are shown in the Fig. 5. The successful incorporation of propyl amine and the formation of succinamic acid over MCM-41 material as well as complete surfactant removal were confirmed. The  $^{13}\text{C}$  CP MAS NMR spectrum of A-MCM-41 (Fig. 5a) revealed the presence of three carbon atoms from the propyl amine group. The sharp peaks at 9.2, 22.1 and 42.9 ppm corresponding to the methylene groups of the propyl chain and were numbered 1, 2 and 3, respectively. The successful formation of succinamic acid over MCM-41 is confirmed in Fig. 5b.

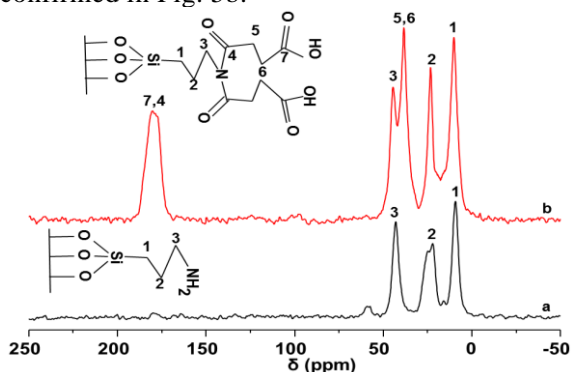


Fig. 5.  $^{13}\text{C}$  CP MAS NMR spectra of (a) A-MCM-41 and (b) SA-MCM-41.

The resonances responsible for the propyl group persisted in the spectrum of SA-MCM-41 with a slight change in positions at 10.1, 23.3 and 44.6 ppm, indicating the functional integrity of the material. The 5<sup>th</sup> and 6<sup>th</sup> carbon resonance merged due to the identical environment and observed at 38.4 ppm. The broad and strong peak was observed at 177 to 180 ppm is responsible for the two carbonyl carbon atoms persisted in the succinamic acid and it's numbered as 4 and 7. Both the major signals of A-MCM-41 and SA-MCM-41 were observed in the spectra and the absence of resonances responsible for the surfactant indicates its complete removal

through calcination. The formation of succinamic acid over MCM-41 was also confirmed by CHNS elemental analysis, and the loading was found to be 5.4 and 1.4 wt% for carbon and nitrogen, respectively [16]. These two analyses resemble the formation of succinamic by the replacement of two hydrogen atoms at the amine functionality [38, 39].

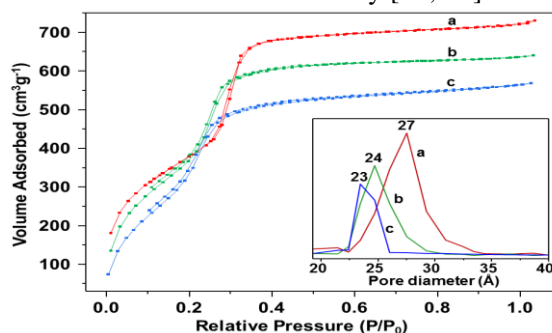


Fig. 6.  $\text{N}_2$  adsorption-desorption isotherms and pore diameter (inset) of (a) MCM-41, (b) A-MCM-41 and (c) SA-MCM-41.

The nitrogen adsorption-desorption isotherms of (a) MCM-41, (b) A-MCM-41 and (c) SA-MCM-41 materials in Fig. 6. All the isotherms were type IV with H1 hysteresis, which shows a typical mesoporous solid, according to the IUPAC classification [40]. The amount of  $\text{N}_2$  adsorbed on all the functionalized samples was lower than the parent MCM-41, which was reflected in the surface areas. The BET surface areas of MCM-41, A-MCM-41 and SA-MCM-41 were 1008, 935 and 809  $\text{m}^2\text{g}^{-1}$ , respectively [16]. The inset of Fig. 6 shows a narrowly distributed pore diameter, which decreased in the order of 27, 24 and 23 Å for MCM-41, A-MCM-41 and SA-MCM-41, respectively. The mesoporous structure persisted, even after two step functionalization on the silica surface.

### B. Adsorption from individual metal solution

Adsorption processes are normally considered intermolecular interactions between the metal and solid surfaces. Electrostatic interactions, hydrogen bonding, weak Van der Waals force of attraction, even complexation are the mode of adsorption of metal ions from the solution to an organic functionalised material. The factors such as pH, contact time, initial ionic strength, and adsorbent dosage strongly dependent on the adsorption efficiency of the material. Consequently, it is necessary to determine the effects of such factors on the adsorption nature and mechanism during the adsorption process. The initial solution pH is an important factor affecting the adsorption of heavy metal ions by influencing the surface charge of the adsorbents and the metal ions in

solution. Therefore, initially a study was conducted to optimize the pH with the other parameters, such as the SA-MCM-41 dose, metal ion concentration and contact time were kept constant.

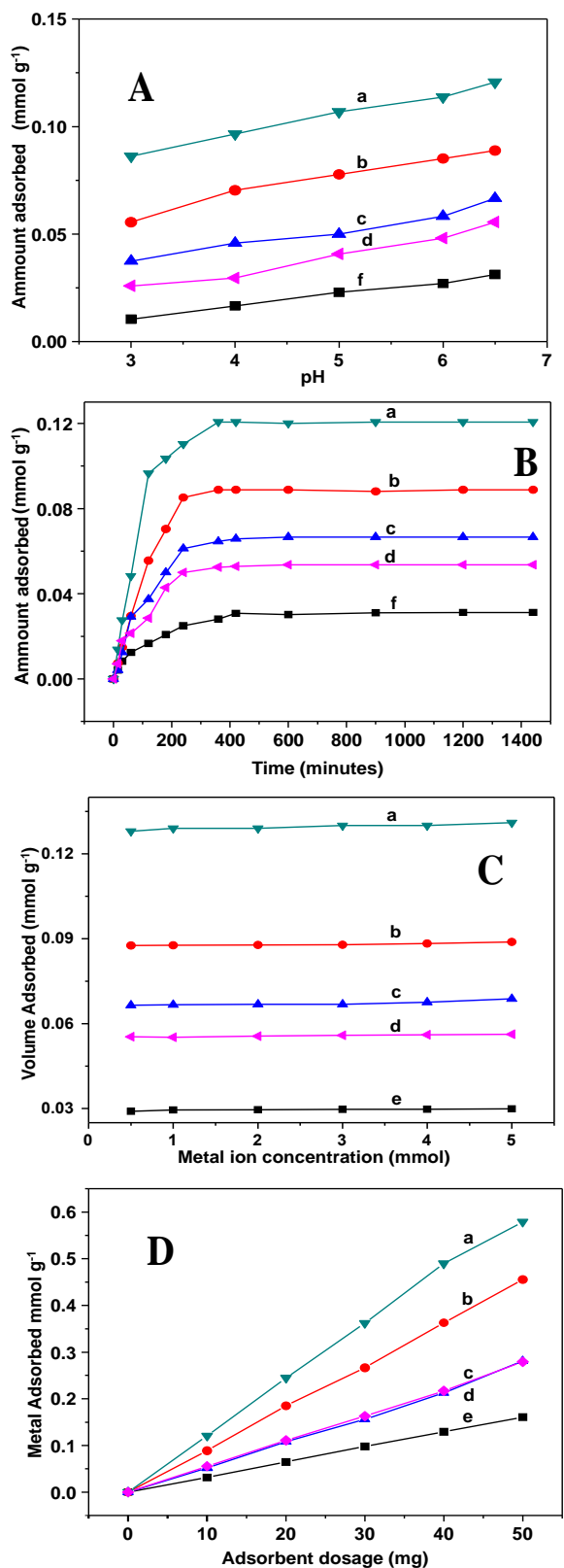


Fig. 7. Effect of various factors on Cd<sup>2+</sup>/Co<sup>2+</sup>/Cr<sup>3+</sup>/Cu<sup>2+</sup>/Ni<sup>2+</sup> adsorption; (A) pH of the

metal solution (concentration: 0.5 mM, adsorbate volume: 10 ml, adsorbent dosage: 0.01 g, time: 24 h), (B) stirring time (concentration: 0.5 mmol, adsorbate volume: 10.0 ml, adsorbent dosage: 0.01 g, pH: 6.5), (C) initial metal ion concentration (adsorbate volume: 10.0 ml, adsorbent dosage: 0.01 g, pH: 6.5, time: 6 h) and (D) adsorbent dosage (concentration: 0.5 mM, adsorbate volume: 10.0 ml, pH: 6.5, time: 6 h).

### 1) Effect of pH

The initial solution pH is an important factor affecting the adsorption of heavy metal ions; because it not only influences the surface charge of the adsorbents, but also the type of metal ions in solution. Therefore, a study was conducted to optimise the pH with the other parameters, such as the SA-MCM-41 dose, metal ion concentration and contact time were kept constant. The effects of pH on the adsorption of Cd<sup>2+</sup>, Co<sup>2+</sup>, Cr<sup>3+</sup>, Cu<sup>2+</sup>, and Ni<sup>2+</sup> from water samples was studied over the pH range, 3 - 6.5, for initial concentrations of 0.5 mM onto SA-MCM-41, as illustrated in Fig. 7A. Higher pH solutions were not able to study due to the precipitation limitation of some metal ions and the instability of functionalised mesoporous silicates in alkali solutions. Adsorption was carried out using 10 ml of each metal solution and 10 mg of SA-MCM-41 for 24 h shaken in a mechanical shaker. Fig. 7A presents the metal adsorption in mmol with respect to per gram SA-MCM-41. The amount of metal adsorption was calculated by the help of ICP-AES analyzer and the adsorption respect to per gram of SA-MCM-41 were 0.010, 0.016, 0.022, 0.027, and 0.031 mmol for Cd<sup>2+</sup>, 0.055, 0.070, 0.077, 0.085, and 0.088 mmol for Co<sup>2+</sup>, 0.037, 0.045, 0.050, 0.058, and 0.066 mmol for Cr<sup>3+</sup>, 0.086, 0.096, 0.106, 0.113, and 0.120 mmol for Cu<sup>2+</sup> and 0.025, 0.029, 0.040, 0.048, and 0.055 mmol, respectively, at pH 3, 4, 5, 6, and 6.5. [41]. All five metal ions exhibited similar adsorption behaviour over the entire pH range but it shown gradual increase directly proportional to solution pH. As shown in the figure, the adsorption capacity was increased considerably when the pH was increased from 3 to 6.5. This can be explained by the protonation effect of H<sup>+</sup> ions present at higher concentrations in solution on the N and O atoms of the SA-MCM-41 adsorbent. At very low solution pH, the concentration of H<sup>+</sup> ions in adsorption medium is very high, which was competing directly with the heavy metal ions for active binding sites [42]. Additionally, due to the smaller size of the H<sup>+</sup> than metal ions it can approach the ligand atoms very easily. As a result, the adsorption of metal ions will decrease with respect to an increase of the acidic strength in the solution. At higher pH, the surface of the adsorbent had a higher negative charge, resulting in higher attraction towards the cations. As an explanation, SA-MCM-41

adsorbed  $\text{Cd}^{2+}$ ,  $\text{Cu}^{2+}$ ,  $\text{Co}^{2+}$ ,  $\text{Ni}^{2+}$ , and  $\text{Zn}^{2+}$  ions from the aqueous solutions with a maximum of 0.027, 0.088, 0.066, 0.120, and 0.055  $\text{mmol g}^{-1}$ , respectively at pH 6.5. At very high pH, metal hydroxides are formed, which resulted in precipitation; therefore, the separation may not have been achieved due to adsorption. When the pH was increased from 3 to 6.5, the removal efficiency of SA-MCM-41 for  $\text{Cd}^{2+}$ ,  $\text{Co}^{2+}$ ,  $\text{Cr}^{3+}$ ,  $\text{Cu}^{2+}$ , and  $\text{Ni}^{2+}$  was increased from 2 to 6, 11 to 18, 8 to 13, 17 to 24, and 5 to 11 %, respectively. To explain this observation, at  $\text{pH} < 7$ , all the metal ions in solution exist as  $\text{M}^{n+}$ . Therefore, most ions are accessible to the adsorbent at a pH near to neutral condition, resulting in an increase in removal efficiency [43].

## 2) Effect of contact time

To determine the suitable contact time for the maximum removal efficiency of SA-MCM-41, the equilibrium contact time was examined. A 0.01 g sample of SA-MCM-41 was suspended in a  $\text{Cd}^{2+}/\text{Co}^{2+}/\text{Cr}^{3+}/\text{Cu}^{2+}/\text{Ni}^{2+}$  solution (10 ml, 0.5 mM) and the mixture was stirred mechanically at 25 °C for different times intervals with a maximum of 0.25 to 24 h at pH 6.5. Subsequently, the mixture was filtered and the concentration of heavy metal ions remaining in solution was determined by ICP-AES. Plots of the amount of adsorption versus stirring time (Fig. 7B) suggested that the adsorption of all metal ions increased with time. All five metal ions showed adsorption equilibrium within 6 h. The reasonably fast kinetics of the matrix-metal ions interaction reflects the good accessibility of the chelating sites of the modified matrix and high binding ability of the metal ions [44].

## 3) Effect of metal ion concentration

The metal ion removal efficiency by a mesoporous material depends greatly on the bonding strategy between the metal ion and the donor atoms of the anchored molecule on the surface. In addition, the adsorption equilibrium can be altered in the adsorbent or adsorbate by merely altering the concentration of metal ions. To examine the effects of the initial metal ion concentration, a 0.01 g sample of SA-MCM-41 was suspended in 10 ml of  $\text{Cd}^{2+}/\text{Co}^{2+}/\text{Cr}^{3+}/\text{Cu}^{2+}/\text{Ni}^{2+}$  solution with a concentration in the range, 0.25 to 5 mM, at pH 6.5. The mixture was stirred mechanically at 25 °C for 6 h. The mixture was filtered and the concentration of heavy metal ions remaining in solution was determined by ICP-AES. Fig 7C shows the amount of  $\text{Cd}^{2+}/\text{Co}^{2+}/\text{Cr}^{3+}/\text{Cu}^{2+}/\text{Ni}^{2+}$  ion adsorption as a function of the initial metal ion concentration in solution. The change in the initial metal ion concentration had a significant effect on the removal efficiency [45]. At low metal ion concentrations, the ratio of surface active sites to the total metal ions in

the solution was high; hence a major portion of the metal ions in solution may interact with the adsorbent and be removed from solution. At higher initial metal ion concentrations, there was a slight increase in the amount of adsorption. On the other hand the rate of the increase in adsorption was reduced at very high initial concentrations. In contrast, SA-MCM-41 could adsorb a maximum of 0.03, 0.09, 0.07, 0.13 and 0.06  $\text{mmol g}^{-1}$  for  $\text{Cd}^{2+}$ ,  $\text{Cu}^{2+}$ ,  $\text{Co}^{2+}$ ,  $\text{Ni}^{2+}$ , and  $\text{Zn}^{2+}$  ions, respectively, from aqueous metal solutions with an initial metal ion concentration of 5 mM. The slower rate of increase in adsorption is the result of the adsorption/desorption equilibrium achieved between metal ions in solution and the adsorbent [28, 34].

## 4) Effect of adsorbent dosage

Fig. 7D shows the effects of the adsorbent (SA-MCM-41) dosage on the adsorption efficiency of  $\text{Cd}^{2+}/\text{Co}^{2+}/\text{Cr}^{3+}/\text{Cu}^{2+}/\text{Ni}^{2+}$  at pH 6.5. There were selected the adsorbent dosage are 0.01, 0.02, 0.03, 0.04, and 0.05 g for the uptake of  $\text{Cd}^{2+}/\text{Co}^{2+}/\text{Cr}^{3+}/\text{Cu}^{2+}/\text{Ni}^{2+}$  from an initial metal ion solution of 0.5 mM. The percentage of removal increased rapidly with SA-MCM-41 dosage about 6, 14, 20, 26, and 32 % for  $\text{Cd}^{2+}$  ion 18, 37, 53, 73 and 91 % for  $\text{Co}^{2+}$  ion 10, 22, 31, 43, and 56 for  $\text{Cu}^{3+}$  ions the  $\text{Cu}^{2+}$  ions progress as 24, 49, 72, 98, and 100 the SA-MCM-41 adsorbent adsorbed the  $\text{Ni}^{2+}$  as 11, 22, 32, 43, and 56 %. The percentage removal was increased from 6 to 32, 17 to 91 and 10 to 56, 24 to 100, and 11 to 56 % for  $\text{Cd}^{2+}$ ,  $\text{Co}^{2+}$ ,  $\text{Cr}^{3+}$ ,  $\text{Cu}^{2+}$ , and  $\text{Ni}^{2+}$ , respectively. When the adsorbent dosage was increased from 0.01 to 0.05 g consequently increases the active functional groups for the uptake of metal ions onto the SA-MCM-41 surface, which results in a high removal percentage. The maximum removal of 100 % was achieved for  $\text{Cu}^{2+}$  at a dose of 0.05 g SA-MCM-41. The maximum removal of 0.16, 0.45, 0.28, 0.58 and 0.28  $\text{mmol g}^{-1}$  were achieved for  $\text{Cd}^{2+}$ ,  $\text{Co}^{2+}$ ,  $\text{Cr}^{3+}$ ,  $\text{Cu}^{2+}$ , and  $\text{Ni}^{2+}$ , respectively, when 0.05 g of adsorbent was used. These results also showed that the metal removal percentage is strongly dependent on the optimal increase in adsorbent dose, due to a consequential increase in interference between the binding sites at the higher dose or an insufficiency of metal ions in solution with respect to the available binding sites [47].

## C. Adsorption of metal ions from metal mixture

Finally, adsorption from metal mixture was carried out to study the adsorption behaviour from a mixture of metal. The metal mixture with individual metal concentration as 0.5 mM for  $\text{Cd}^{2+}$ ,  $\text{Co}^{2+}$ ,  $\text{Cr}^{3+}$ ,  $\text{Cu}^{2+}$ , and  $\text{Ni}^{2+}$  and the adsorption result was illustrated in the Fig. 8. 10 ml of the above solution was mixed with 0.01 g of the SA-MCM-41 and shaken for 12 h to achieve the adsorption equilibrium. Fig. 8 illustrated the adsorption from mixture metal solution suggested that the adsorption of all metal ions increased with time.

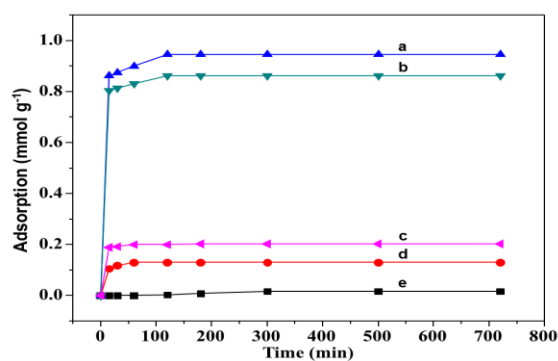


**Fig. 8** Adsorption kinetics of metal mixture (a =  $\text{Cd}^{2+}$ , b =  $\text{Co}^{2+}$ , c =  $\text{Cr}^{3+}$ , d =  $\text{Cu}^{2+}$ , and e =  $\text{Ni}^{2+}$ ). Metal concentration: 0.5 mM, adsorbate volume: 10 ml, adsorbent dosage: 0.01 g, time: 12 h).

All five metal ions showed adsorption equilibrium within 4 h. The reasonably fast kinetics of the matrix–metal ions interaction reflects the good accessibility of the chelating sites of the modified matrix and high binding ability of the metal ions [47].

The ICP-AES result shows the adsorption for five metals in solution were observed like the SA-MCM-41 is almost inactive for  $\text{Cd}^{2+}$  ions in the mixture. The result showed the SA-MCM-41 adsorption maximum is 0.017, 0.130, 0.946, 0.862, and 0.204 mmol, respectively for  $\text{Cd}^{2+}$ ,  $\text{Co}^{2+}$ ,  $\text{Cr}^{3+}$ ,  $\text{Cu}^{2+}$ , and  $\text{Ni}^{2+}$ . The SA-MCM-41 exhibited a higher affinity towards  $\text{Cr}^{3+}$  and  $\text{Cu}^{2+}$  ions, when considering the amount in mmol [40, 47]. The calculated result for amount of adsorption as 0, 4, 23, 25, and 6  $\text{mg g}^{-1}$ , respectively for  $\text{Cd}^{2+}$ ,  $\text{Co}^{2+}$ ,  $\text{Cr}^{3+}$ ,  $\text{Cu}^{2+}$ , and  $\text{Ni}^{2+}$ . There is observed an unusual property in the cause of percentage of adsorption that the high amount of removal for  $\text{Cr}^{3+}$  and  $\text{Cu}^{2+}$ , respectively as 95 and 94 %. But the observed percentage of adsorption for  $\text{Cd}^{2+}$ ,  $\text{Co}^{2+}$  and  $\text{Ni}^{2+}$  as 0, 14 and 20, respectively from metal mixture.

The adsorption efficiency of SA-MCM-41 from the metal mixture showed an unusual adsorption property as compared with individual metal solution. The adsorption experiment with individual metal solution was shown very less affinity towards SA-MCM-41. The adsorption from individual metal solution and metal mixture shown there is no adsorption for  $\text{Cd}^{2+}$  ions. The another important observation is the tremendous increases in the amount of adsorption from 5 to 95 % for  $\text{Cr}^{3+}$  and 12 to 94 % for  $\text{Cu}^{2+}$ . The molar adsorption selectivity from aqueous mixtures will be always a factor of the nature of the ligand, chelation effect, ionic size, and ionic potential (charge to radius ratio) of metal ions. This observed adsorption fortiori complexation ability of the carboxylic acid in combination with nitrogen result the massive adsorption. A chelated complex will be always stable due to the significant gain in entropy. As a result, the succinamic acid functionalized MCM-41 can adsorb metal ions more strongly and efficiently from metal mixture solution.

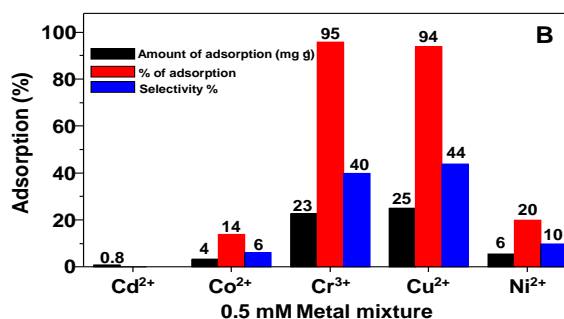
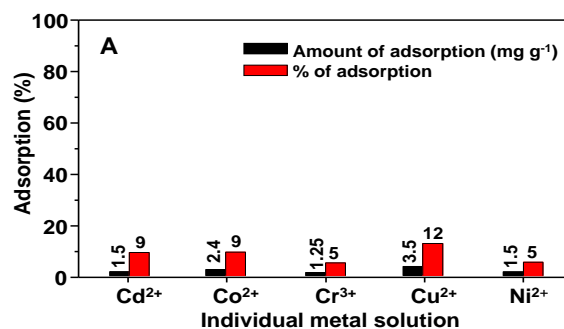


**Fig. 9.** Comparison of metal adsorption by SA-MCM-41 from (A) individual metal solution (B) metal mixture. Metals:-  $\text{Cd}^{2+}$ ,  $\text{Co}^{2+}$ ,  $\text{Cr}^{3+}$ ,  $\text{Cu}^{2+}$ , and  $\text{Ni}^{2+}$ . Concentration: 0.5 mM, adsorbate volume: 10 ml, adsorbent dosage: 0.01 g, time: 12 h).

The Fig. 9 visualized the comparison of adsorption efficiency of SA-MCM-41 from individual and metal mixture solutions. The amount of adsorption (mg) is comparatively very low from individual metal solution (Fig. 9A). The percentage of adsorption obtained as 9, 9, 5, 12, and 5 %, respectively for  $\text{Cd}^{2+}$ ,  $\text{Co}^{2+}$ ,  $\text{Cr}^{3+}$ ,  $\text{Cu}^{2+}$ , and  $\text{Ni}^{2+}$ , from individual metal solution. In the case of adsorption from metal mixture (Fig. 9B) clearly evident the difference as the increases in amount of adsorption and the result introduces a new outcome as the adsorption selectivity among metal ions. Even though, the selectivity is not much promising by this adsorption study, the percentage of adsorption above 90 % for  $\text{Cr}^{3+}$  and  $\text{Cu}^{2+}$  ions from the metal mixture shown the unresolved performance of the new material. The comparison of two adsorption results revealed the combination of metal ions can play a role of adsorption performance of a silane functionalized material. The calculated result for amount of adsorption as 0, 4, 23, 25, and 6  $\text{mg g}^{-1}$ , respectively for  $\text{Cd}^{2+}$ ,  $\text{Co}^{2+}$ ,  $\text{Cr}^{3+}$ ,  $\text{Cu}^{2+}$ , and  $\text{Ni}^{2+}$ . There is observed an unusual property in the cause of percentage of adsorption that the high amount of removal for  $\text{Cr}^{3+}$  and  $\text{Cu}^{2+}$ , respectively as 95 and 93 %. But the observed percentage of adsorption for  $\text{Cd}^{2+}$ ,  $\text{Co}^{2+}$  and  $\text{Ni}^{2+}$  as 0, 16 and 20, respectively from metal mixture.

#### ACKNOWLEDGMENT

The authors are thankful to the Chungnam National University, Korea Basic Science Institute

and Pusan National University, South Korea for characterizing the materials.

#### IV. CONCLUSION

In summary, succinamic acid functionalized MCM-41 was successfully utilized for the adsorption of selected transition metals. A good adsorbent should have high specific surface area, high ligation capacity and high surface adsorption density. SA-MCM-41 satisfies all these characteristics. Also, the adsorption conditions like pH, contact time, metal ion concentration and adsorbent dosage were played a key role in the performance of the adsorbent. The material showed exceptional adsorption ability  $\text{Cr}^{3+}$  and  $\text{Cu}^{2+}$  ions from the five metal mixture at pH 6.5.

#### REFERENCES

- [1] C. T. Cresge, M. E. Leonowicz, W. J. Roth, and J. C. Vartuli, *J. S. Beck, Nature* 359, 710 (1992).
- [2] J. S. Beck, J. C. Vartuli, W. J. Roth, M. E. Leonowicz, C. T. Kresge, K. D. Schmitt, C. T. W. Chu, D. H. Olson, E. W. Sheppard, S. B. McCullen, J. B. Higgins, and J. L. Schlenker, *J. Am. Chem. Soc.* 114, 10834 (1992).
- [3] A. Mathew, S. Parambadath, M. J. Barnabas, S. Y. Kim, D. W. Kim, K. M. Rao, S. S. Park, and C. S. Ha, *Micropor. Mesopor. Mater.* 238 (2017) 27-35.
- [4] E. Dána, *Micropor. Mesopor. Mater.* 247 (2017) 145.
- [5] F. Hoffmann, M. Cornelius, J. Morell, and M. Fröba, *Angew. Chem. Int. Ed.*, 45 (2006) 3216-3251.
- [6] M. S. Moorthy, P. K. Tapaswi, S. S. Park, A. Mathew, H. J. Cho, and C. S. Ha, *Micropor. Mesopor. Mater.* 180 (2013) 162-171.
- [7] C. S. Griffith, V. Luca, J. Cochrane, and J. V. Hanna, *Micropor. Mesopor. Mater.* 111 (2008) 387.
- [8] F. M. Koehler, M. Rossier, M. Waelle, E. K. Athanassiou, L. G. Limbach, R. N. Grass, D. Gunther, and W. J. Stark, *Chem. Commun.* 32 (2009) 4862.
- [9] H. Yang, N. Coombs, I. Sokolova, and G. A. Ozin, *J. Mater. Chem.* 7 (1997) 1285.
- [10] S. Parambadath, A. Mathew, S. S. Park, and C. S. Ha, *J. Environ. Chem. Eng.* 3 (2015) 1918-1927.
- [11] V. Hernández-Morales, R. Nava, Y. J. Acosta-Silva, S. A. Macías-Sánchez, J. J. Pérez-Bueno, and B. Pawelec, *Micropor. Mesopor. Mater.* 160 (2012) 133-142.
- [12] K.M. Parida, and D. Rath, *J. Molecular Catalysis A: Chemical* 310 (2009) 93-100.
- [13] A. Datt, I. El-Maazawi, and S. C. Larsen *J. Phys. Chem. C* 2012, 116, 18358-18366.
- [14] G. E. Fryxell, S. V. Mattigod, Y. Lin, H. Wu, S. Fiskom, K. Parker, F. Zheng, W. Yantasee, T. S. Zemanian, R. S. Addleman, J. Liu, K. Kemner, S. Kelly, X. Feng, *J. Mater. Chem.* 17 (2007) 2863-2874.
- [15] B. D. Lourdes, N. R. David, C. C. Mercedes, *Chem. Soc. Rev.* 36 (2007) 993-1017.
- [16] A. Mathew, S. Parambadath, M. J. Barnabas, H. J. Song, J. S. Kim, S. S. Park, C. S. Ha, *Dyes Pigm.* 131 (2016) 177-185.
- [17] A. Mathew, S. Parambadath, S. Y. Kim, H. M. Ha, C. S. Ha, *Micropor. Mesopor. Mater.* 229 (2016) 124-133.
- [18] T. Ukmar, U. Maver, O. Planinsek, A. Pintar, V. Kaucic, A. Godec, et al., *J. Mater. Chem.* 22 (2012) 1112-1120.
- [19] K. Ananthanarayanan, P. Natarajan, *Micropor. Mesopor. Mater.* 124 (2009) 179-189.
- [20] J. Kobler, K. Möller, T. Bein, *ACS Nano* 2 (2008) 791-799.
- [21] A. C. Pradhan, K. M. Parida, *J. Mater. Chem.* 22 (2012) 7567-7579.
- [22] D. P. Quintanilla, A. Sanchez, I. dei Hierro, M. Fajardo, I. Sierra, *J. Coll. Inter. Sci.* 313 (2007) 551-562.
- [23] A. Mathew, S. Parambadath, S. Y. Kim, S.S. Park, C.S. Ha, *J Porous Mater* 22 (2015) 831-842.
- [24] S. Radi, S. Tighadouini, M. El Massaoudi, M. Bacquet, S. Degoutin, B. Revel, Y. N. Mabkhot, *J. Chem. Eng. Data* 60 (2015) 2915-2925.
- [25] A. C. Pradhan, K. M. Parida, *J Mater Chem*, 22 (2012) 7567-7579.
- [26] S. Ray, M. Brown, A. Bhaumik, A. Dutta, C. Mukhopadhyay, *Green Chem.* 15 (2013) 1910-1924.
- [27] C. Y. Lai, B. G. Trewyn, D. M. Jefstiniya, K. Jefstiniya, S. Xu, S. Jefstiniya, *J. Am. Chem. Soc.* 125 (2003) 4451-4459.
- [28] I. Slowing, B. G. Trewyn, V. S. Y. Lin, *J. Am. Chem. Soc.* 128 (2006) 14792-14793.
- [29] E. Moazzen, N. Daei, S. M. Hosseini, H. Ebrahimzadeh, A. Monfared, M. M. Amini, O. Sadeghi, *Microchim Acta* 178 (2012) 367-372.
- [30] H. Ebrahimzadeh, N. Tavassoli, O. Sadeghi, M. M. Amini, S. Vahidi, S. M. Aghigh, E. Moazzen, *Food Anal Methods* 5 (2012) 1070-1078.
- [31] M. A. Qunaibit, M. Khalil, A. A. Wassil, *Chemosphere* 60 (2005) 412-418.
- [32] M. R. Jamalia, Y. Assadi, Shemirani F, M. S. Niasari, *Talanta* 71 (2007) 1524-1529.
- [33] A. Bagheri, M. Taghizadeh, M. Behbahani, A. A. Asgharinezhad, M. Salarian, A. Dehghani, H. Ebrahimzadeh, M. M. Amini, *Talanta* 99 (2012) 132-139.
- [34] V. Kumari, M. Sasidharan, A. Bhaumik, *Dalton Trans.* 44 (2015) 1924-1932.
- [35] S. Parambadath, A. Mathew, M. J. Barnabas, K. M. Rao, C. S. Ha, *Micropor. Mesopor. Mater.* 225 (2016) 174-184.
- [36] V. K. Rana, M. Selvaraj, S. Parambadath, C. S. Wook, S. S. Park, S. Mishra, *J. Solid State Chem.* 194 (2012) 392-399.
- [37] M. D. Popova, A. Szegedi, I. N. Kolev, J. Mihaly, B. S. Tzankov, G. M. Tz, *Int. J. Pharm* 436 (2012) 778-785.
- [38] P. Kumar, V. V. Gulians, *Micropor. Mesopor. Mater.* 132 (2010) 1-14.
- [39] D. P. Quintanilla, I. Hierro, M. Fajardo, I. Sierra, *Micropor. Mesopor. Mater.* 89 (2006) 58-68.
- [40] A. Mathew, S. Parambadath, S.S. Park, C.S. Ha, *Micropor. Mesopor. Mater.* 200 (2014) 124-131.
- [41] F. Gode, E. Pehlivan, *J. Hazard. Mater.* 136 (2006) 330-337.
- [42] P. Govindaraj, P. Sivasamy, J. Rejinis, *J. Chem. Pharma. Res.* 2012, 4, 286-293.
- [43] G. L. Radu, G. I. Truica, R. Penu, V. Moroceanu, S. C. Litescu, *UPB Sci. Bull. Ser. B* 74 (2012) 137-148.
- [44] M. S. Moorthy, S. S. Park, M. Selvaraj, C. S. Ha, *J. Nanosci. Nanotechnol.* 14 (2014) 8891-8897.
- [45] A. Bagheri, M. Behbahani, M. M. Amini, O. Sadeghi, M. Taghizade, L. Baghayi, M. Salarian, *Talanta* 89 (2012) 455-461.
- [46] A. Bagheri, M. Taghizadeh, M. Behbahani, A. A. Asgharinezhad, M. Salarian, A. Dehghani, H. Ebrahimzadeh, M. M. Amini, *Talanta* 99 (2012)132-139.
- [47] S. Parambadath, A. Mathew, M. J. Barnabas, S. Y. Kim, C. S. Ha, *J Sol-Gel Sci Technol*, (2015) DOI 10.1007/s10971-015-3923-x